NMR relaxation in Ising spin chains

Julia Steinberg, N. P. Armitage, Fabian H. L. Essler, and Subir Sachdev

NMR relaxation in Ising spin chains

Julia Steinberg,[1] N. P. Armitage,[2] Fabian H.L. Essler,[3] and Subir Sachdev[1,4]

[1]*Department of Physics, Harvard University, Cambridge MA 02138, USA*

[2]*The Institute for Quantum Matter, Department of Physics and Astronomy,*
The Johns Hopkins University, Baltimore, MD 21218 USA

[3]*Rudolf Peierls Centre for Theoretical Physics, Parks Road, Oxford OX1 3PU, UK*

[4]*Perimeter Institute for Theoretical Physics,*
Waterloo, Ontario, Canada N2L 2Y5

(Dated: November 9, 2018)

Abstract

We examine the low frequency spin susceptibility of the paramagnetic phase of the quantum Ising chain in transverse field at temperatures well below the energy gap. We find that the imaginary part is dominated by rare quantum processes in which the number of quasiparticles changes by an odd number. We obtain exact results for the NMR relaxation rate in the low temperature limit for the integrable model with nearest-neighbor Ising interactions, and derive exact universal scaling results applicable to generic Ising chains near the quantum critical point. These results resolve certain discrepancies between the energy scales measured with different experimental probes in the quantum disordered paramagnetic phase of the Ising chain system $CoNb_2O_6$.

I. INTRODUCTION

The transverse field Ising chain is an ideal setting to study the dynamics of quantum criticality [1] as many observable properties can be computed either exactly, or reliably in a semiclassical approach [2–4]. In recent years, there have been several experimental realizations of the transverse Ising chain that make theoretical predictions testable [5, 6]. For instance, it has been found that $CoNb_2O_6$ is for many purposes an almost ideal realization of the one-dimensional ferromagnetic Ising chain. Experiments have studied its properties across the different regimes of the phase diagram as a function of transverse field and temperature [5, 7–11].

In this paper, we revisit the issue of the nuclear magnetic resonance (NMR) relaxation in an Ising spin chain in its gapped state without ferromagnetic order (the 'quantum disordered' regime of Fig. 1). A recent NMR experiment on $CoNb_2O_6$ [8] studied the NMR relaxation rate, $1/T_1$, in all three regimes near the quantum critical point of the phase diagram in Fig. 1. Experimental results agreed quantitatively with theoretical predictions in the 'renormalized classical' and 'quantum critical' regimes. While there were no firm theoretical predictions in the quantum disordered regime, it was conjectured [8] that the low temperature (T) behavior was $1/T_1 \sim \exp(-\Delta/T)$, where Δ is the energy gap to single spin flips. However, other experiments probing the large field transverse paramagnetic regime show discrepancies with the energy scales probed by NMR. The NMR experiments [8] measured an activation energy that was approximately two times larger than the gap inferred from heat capacity [10], neutron scattering [11], and THz/infrared experiments [12].

Here we will show that near the critical point the behavior of the NMR relaxation rate is in fact $1/T_1 \sim \exp(-2\Delta/T)$, and compute the precise prefactor for the integrable nearest-neighbor Hamiltonian. We find that the result is compatible with the universal relativistic quantum field theory, and obtain the universal behavior of $1/T_1$ at $T \ll \Delta$ for a generic Ising Hamiltonian. We begin by recalling some exact results on the nearest-neighbor Ising chain in Section II. In particular, the lattice form factors computed in Ref. 4 will be crucial ingredients in our results. The computation of the NMR relaxation rate of the nearest-neighbor Ising chain appears in Section III. Section IV describes the universal behavior of the NMR relaxation rate across the quantum critical point. The experimental situation is discussed in Section V.
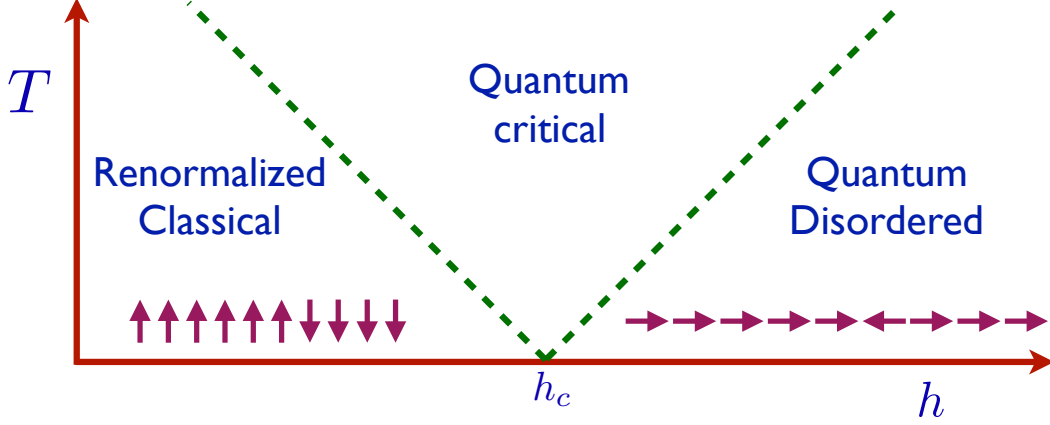
2

FIG. 1. Crossover phase diagram of the Ising chain in a transverse field, h. There is a quantum critical point at $T = 0$ and $h = h_c$ (for the Hamiltonian in Eq. (2.1), $h_c = 1$) between a ferromagnetic ($h < h_c$) which breaks the Ising symmetry, and a paramagnetic phase. This paper focuses on the "quantum disordered" regime above the paramgetic phase for $h > h_c$. The other regimes were described in Ref. 8.

II. EXACT SPECTRUM

We work with the integrable Ising chain Hamiltonian

$$H = -J \sum_{\ell=1}^{L} \left[\sigma_\ell^z \sigma_{\ell+1}^z + h \sigma_\ell^x \right] \tag{2.1}$$

where $\sigma_\ell^{x,z}$ are Pauli matrices acting on the 2-state spins on site ℓ. For $h < 1$, this model has a ferromagnetic ground state with $\langle \sigma_\ell^z \rangle = N_0 \neq 0$. We are interested in the low T behavior in the paramagnetic state for $h > 1$, where $\langle \sigma_\ell^z \rangle = 0$ at $T = 0$.

The spectrum of H can be computed exactly by a Jordan-Wigner transformation which maps it onto a theory of spinless fermions with dispersion

$$\varepsilon_p = 2J\sqrt{1 + h^2 - 2h\cos(p)} \tag{2.2}$$

as a function of crystal momentum $-\pi < p < \pi$. This dispersion implies an energy gap

$$\Delta = 2J|h - 1|. \tag{2.3}$$

The complete set of excited states are described by n fermion states $|p_1, p_2, \ldots, p_n\rangle$, where all fermion momenta must be unequal.

Remarkably, all matrix elements of the ferromagnetic order parameter, σ_ℓ^z, between all many-body states have been computed exactly by Iorgov *et al.* [4]. For our purposes, we need the matrix

3

elements in the limit $L \to \infty$, which can be written as

$$\langle q_1, \ldots, q_{2n} | \sigma_\ell^z | p_1, \ldots, p_m \rangle = \frac{(4J^2h)^{(m-2n)^2/4}}{L^{n+m/2}} |1 - h^2|^{1/8} i^{\lfloor n+m/2 \rfloor} e^{-i\ell \left[\sum_{j=1}^{2n} - \sum_{l=1}^{m} p_l \right]}$$

$$\times \prod_{j=1}^{2n} \frac{1}{\sqrt{\varepsilon_{q_j}}} \prod_{l=1}^{m} \frac{1}{\sqrt{\varepsilon_{p_l}}} \prod_{j<j'=1}^{2n} \frac{2\sin(q_j - q_{j'})}{\varepsilon_{q_j} + \varepsilon_{q_{j'}}} \prod_{l<l'=1}^{m} \frac{2\sin(p_l - p_{l'})}{\varepsilon_{p_l} + \varepsilon_{p_{l'}}} \prod_{j=1}^{2n}\prod_{l=1}^{m} \frac{\varepsilon_{q_j} + \varepsilon_{p_l}}{2\sin(q_j - p_l)}, \quad (2.4)$$

where m is even (odd) for $h < 1$ ($h > 1$). We will be able to compute the NMR relaxation rate in the $T \to 0$ limit for $h > 1$ by a direct application of Eq. (2.4) in the Lehmann spectral representation.

III. NMR RELAXATION RATE

The NMR relaxation rate is determined by the low frequency behavior of local spin susceptibility. We define the imaginary time (τ) susceptibility by

$$\chi(\tau) = \int_0^{1/T} d\tau \, \langle \sigma_0^z(\tau) \sigma_0^z(0) \rangle \, . \quad (3.1)$$

After a Fourier transform and analytic continuation to real frequencies (ω), we obtain the NMR relaxation rate from [8]

$$\frac{1}{T_1} = \lim_{\omega \to 0} \frac{2T}{\omega} |a_{hf}|^2 \text{Im}\chi(\omega) \, , \quad (3.2)$$

where a_{hf} is the hyperfine coupling between the nuclei and the Ising spins.

A. Low-temperature expansion

We are interested in the retarded two-point order parameter autocorrelator

$$\chi(\omega) = \int_0^{1/T} d\tau e^{i\overline{\omega}\tau} \frac{1}{\mathcal{Z}} \text{Tr} \left[e^{-H/T} \sigma_j^z(\tau) \sigma_j^z \right] \Bigg|_{\overline{\omega} \to \eta - i\omega}, \quad (3.3)$$

where $\mathcal{Z}$ is the partition function. The idea of Ref. 3 is to develop a linked cluster expansion for this quantity. The starting point is the Lehmann representation

$$\chi(\omega) = \frac{1}{\mathcal{Z}} \sum_{n,m=0}^{\infty} C_{n,m}(\omega) \, , \quad (3.4)$$

where

$$C_{n,m}(\omega) = \frac{1}{n!} \sum_{\{k_1, \ldots k_n\}} \frac{1}{m!} \sum_{\{p_1, \ldots, p_m\}} |\langle k_1 \cdots k_n | \sigma_0^z | p_1 \cdots p_m \rangle|^2 \frac{e^{-E(\{p_i\})/T} - e^{-E(\{k_j\})/T}}{\omega + i\eta - E(\{p_i\}) + E(\{k_j\})} \, . \quad (3.5)$$

4

Here η is a positive infinitesimal. The expansion of the partition function reads

$$\mathcal{Z} = 1 + \sum_{p \in \mathrm{R}} e^{-\varepsilon_p/T} + \sum_{p_1 < p_2 \in \mathrm{NS}} e^{-[\varepsilon_{p_1} + \varepsilon_{p_2}]/T} + \ldots \equiv \sum_{n=0}^{\infty} \mathcal{Z}_n. \qquad (3.6)$$

By construction the contribution $\mathcal{Z}_n$ scales with system size as L^n. Here the subscripts refer to Ramond and Neveu-Schwartz boundary conditions, which will not matter in the infinite L limit we take. The individual terms $C_{n,m}(\omega)$ in the expansion (3.4) diverge with the system size L because the matrix elements (2.4) become singular when $k_r \to p_s$. Ref. 3 re-casts the expansion in terms of *linked clusters*, which are finite in the thermodynamic limit. The linked clusters relevant for a low-temperature expansion of $\chi(\omega)$ are

$$\begin{aligned}
\mathbf{C}_{2n+1,0}(\omega) &= C_{2n+1,0}(\omega) , & \mathbf{C}_{0,2n+1}(\omega) = C_{0,2n+1}(\omega) , \\
\mathbf{C}_{1,2n}(\omega) &= C_{1,2n}(\omega) - \mathcal{Z}_1 C_{0,2n-1}(\omega) , \\
\mathbf{C}_{2,2n+1}(\omega) &= C_{2,2n+1}(\omega) - \mathcal{Z}_1 C_{1,2n}(\omega) - (\mathcal{Z}_2 - \mathcal{Z}_1^2) C_{0,2n-1}(\omega) , \\
\mathbf{C}_{3,2n}(\omega) &= C_{3,2n}(\omega) - \mathcal{Z}_1 C_{2,2n-1}(\omega) - (\mathcal{Z}_2 - \mathcal{Z}_1)^2 C_{1,2n-2}(\omega) .
\end{aligned} \qquad (3.7)$$

In terms of the linked clusters we have

$$\operatorname{Im} \chi(\omega) = \sum_{n,m=0}^{\infty} \operatorname{Im} \mathbf{C}_{n,m}(\omega) . \qquad (3.8)$$

The leading terms at low temperatures and $\omega \approx 0$ are

$$\begin{aligned}
\mathcal{C}_1(\omega) &= \mathbf{C}_{1,2}(\omega) + \mathbf{C}_{2,1}(\omega) , \\
\mathcal{C}_2(\omega) &= \mathbf{C}_{2,3}(\omega) + \mathbf{C}_{3,2}(\omega) , \\
\mathcal{C}_3(\omega) &= \mathbf{C}_{1,4}(\omega) + \mathbf{C}_{4,1}(\omega) + \mathbf{C}_{3,4}(\omega) + \mathbf{C}_{4,3}(\omega) .
\end{aligned} \qquad (3.9)$$

As $\varepsilon_k > \Delta = 2J|h-1|$ the formal temperature dependence of these terms at $T \ll \Delta$ is

$$\mathcal{C}_n(\omega) = \mathcal{O}\big(e^{-(n+1)\Delta/T}\big). \qquad (3.10)$$

As we are interested in the NMR relaxation rate we focus on the quantities

$$c_n(T) = \lim_{\omega \to 0} \frac{\operatorname{Im}\big(\mathcal{C}_n(\omega)\big)}{\omega} . \qquad (3.11)$$

1. Leading term

We begin with some qualitative considerations on the physical processes which lead to the dominant contributions to Eq. (3.2) as $T \to 0$ for $h > 1$. A thermal excitation with energy E_i will

appear with a probability $e^{-E_i/T}$ as an initial state in the relaxation process. We should focus on the states with the lowest possible E_i. Because of the $\omega \to 0$ limit, the final states will also have an energy $E_f = E_i$ and are reached by the action of the σ_0^z operator. We notice from Eq. (2.4) that for $h > 1$ the matrix element is non-zero only between states with distinct parities in the number of fermions. Therefore the initial and final states must differ by an odd number of fermions which places strong constraints on the ranges of allowed values of E_i and E_f.

We first consider the process $1 \to 2$, from an initial state with one fermion to a final state with 2 fermions. This process (and its inverse) will dominate as $T \to 0$. The single fermion excitations are in the energy range $(\varepsilon_{\min}, \varepsilon_{\max}) \equiv 2J(h - 1, h + 1)$. In the most optimal conditions, both fermions in the 2 particle state will have energy close to $\varepsilon_{\min}$. So for a $1 \to 2$ particle process to be allowed, we need $\varepsilon_{\max} > 2\varepsilon_{\min}$ or $h < 3$. This process will have probability $\exp(-2\varepsilon_{\min}/T)$.

For $h > 3$ we need to consider processes with larger numbers of fermions to obtain the leading contribution. In general, the $n \to m$ process is allowed for $h < (m + n)(m - n)$, where $m > n$ and $m - n$ is odd. Such a process occurs with probability $\exp(-m\varepsilon_{\min}/T)$. Thus for $3 < h < 5$ the most probable process is $2 \to 3$ with probability $\exp(-3\varepsilon_{\min}/T)$. There are also processes at smaller h, such as $1 \to 4$ for $h < 5/3$ with probability $\exp(-4\varepsilon_{\min}/T)$.

We now consider the $1 \to 2$ process which has a prefactor of $\exp(-2\Delta/T)$. Importantly for $\omega \approx 0$ and in the limit $\eta \to 0$ we have

$$\lim_{\eta \to 0} \big[\text{Im} \mathcal{C}_1(\omega) \big] = \lim_{\eta \to 0} \text{Im} \big[C_{1,2}(\omega) + C_{2,1}(\omega) \big] \tag{3.12}$$

i.e. the "disconnected" contributions $\mathcal{Z}_1 C_{01}(\omega)$ and $\mathcal{Z}_1 C_{10}(\omega)$ vanish in the limit $\eta \to 0$. This is related to the fact that the kinematic poles in the form factors do not contribute to the momentum sums by virtue of the energy-conservation delta function. Using the explicit expression for the form factors (2.4) and turning momentum sums into integrals in the $L \to \infty$ limit we have

$$\text{Im} \big(\mathcal{C}_1(\omega) \big) = \frac{J\pi}{4} [h^2(h^2 - 1)]^{\frac{1}{4}} \int_{-\pi}^{\pi} \frac{dp_1 dp_2 dq}{(2\pi)^3} \big[\delta(\omega + \varepsilon_{p_1} + \varepsilon_{p_2} - \varepsilon_q) - \delta(\omega - \varepsilon_{p_1} - \varepsilon_{p_2} + \varepsilon_q) \big]$$

$$\times \frac{(\varepsilon_{p_1} + \varepsilon_q)^2 (\varepsilon_{p_2} + \varepsilon_q)^2 \sin^2 \left(\dfrac{p_1 - p_2}{2} \right)}{\varepsilon_{p_1} \varepsilon_{p_2} \varepsilon_q (\varepsilon_{p_1} + \varepsilon_{p_2})^2 \sin^2 \left(\dfrac{p_1 - q}{2} \right) \sin^2 \left(\dfrac{p_2 - q}{2} \right)} \big[e^{-(\varepsilon_{p_1} + \varepsilon_{p_2})/T} - e^{-\varepsilon_q/T} \big] \tag{3.13}$$

Carrying out one of the integrals using the energy conservation delta-function we obtain

$$c_1(T) = \frac{J}{2T} [h^2(h^2 - 1)]^{\frac{1}{4}} \int_{-\pi}^{\pi} \frac{dp_1 dp_2}{(2\pi)^2} \Theta_H \big(2J(h + 1) - \varepsilon_{p_1} - \varepsilon_{p_2} \big) \frac{e^{-(\varepsilon_{p_1} + \varepsilon_{p_2})/T}}{|\varepsilon'_{p_0}|}$$

$$\times \frac{(2\varepsilon_{p_1} + \varepsilon_{p_2})^2 (\varepsilon_{p_1} + 2\varepsilon_{p_2})^2 \sin^2 \left(\dfrac{p_1 - p_2}{2} \right)}{\varepsilon_{p_1} \varepsilon_{p_2} (\varepsilon_{p_1} + \varepsilon_{p_2})^3 \sin^2 \left(\dfrac{p_1 - p_0}{2} \right) \sin^2 \left(\dfrac{p_2 - p_0}{2} \right)}, \tag{3.14}$$

where

$$p_0 = \arccos\left[\frac{1 + h^2 - \left(\frac{\varepsilon_{p_1} + \varepsilon_{p_2}}{2J}\right)^2}{2h}\right]. \tag{3.15}$$

In the low-temperature limit $T \ll 2J(h-1)$ and $h < 3$ we can carry out the remaining two integrals as follows. The integration will be dominated by small $p_{1,2} \sim \sqrt{T}$. For these small p, we can expand the dispersion as

$$\varepsilon_p = \Delta + \frac{p^2}{2m} + \dots \tag{3.16}$$

where $\Delta = 2J(h-1)$ and $m = (h-1)/(2hJ)$. Expanding the rest of the integrand around $p_1 = p_2 = 0$ we obtain

$$c_1(T) = \frac{J}{T}e^{-2\Delta/T}\frac{81[h^2(h^2-1)]^{\frac{1}{4}}}{64|\varepsilon'_{q_0}|\Delta \sin^4(q_0/2)}\int_{-\pi}^{\pi}\frac{dp_1 dp_2}{(2\pi)^2}e^{-\frac{p_1^2+p_2^2}{2mT}}(p_1 - p_2)^2,$$

$$= \frac{81m^2TJ[h^2(h^2-1)]^{\frac{1}{4}}}{64\pi\Delta \sin^4(q_0/2)|\varepsilon'_{q_0}|}e^{-2\Delta/T}, \tag{3.17}$$

where we have defined

$$q_0 = \arccos\left[\frac{1 + h^2 - 4(h-1)^2}{2h}\right]. \tag{3.18}$$

Using Eq. (3.2), we obtain our main result

$$\frac{1}{T_1} = |a_{hf}|^2\left[\frac{81Jm^2[h^2(h^2-1)]^{1/4}}{32\pi\Delta|v|\sin^4(q_0/2)}\right]T^2e^{-2\Delta/T} \quad , \quad 1 < h < 3 \quad , \quad T \ll \Delta. \tag{3.19}$$

Note that Eq. (3.19) does not require Δ to be much smaller than J.

2. Subleading term

We now turn to the term of order $e^{-3\Delta/T}$. For $1 < h < 3$ this will be smaller than the $e^{-2\Delta/T}$ term computed in Sec. III A 1, while for $3 < h < 5$ this turns out to be the largest non-zero term.

We will evaluate

$$c_2(T) = \lim_{\omega \to 0}\frac{\mathrm{Im}\big(\mathcal{C}_2(\omega)\big)}{\omega}. \tag{3.20}$$

This can be cast in the form

$$c_2(T) = \lim_{\eta \to 0}\left[c_2(T, \eta) - \mathcal{Z}_1 c_1(T, \eta) - (\mathcal{Z}_2 - \mathcal{Z}_1^2)c_0(T, \eta)\right], \tag{3.21}$$

where we have defined

$$c_n(T, \eta) = \lim_{\omega \to 0}\mathrm{Im}\left[\frac{C_{n,n+1}(\omega) + C_{n+1,n}(\omega)}{\omega}\right], \quad n = 0, 1, 2, \tag{3.22}$$

7

and $\mathcal{Z}_n$ are the contributions of n-particle states to the partition function

$$\mathcal{Z}_1 = \sum_{p \in \mathrm{R}} e^{-\varepsilon_p/T} \ , \qquad \mathcal{Z}_2 = \sum_{p_1 < p_2 \in \mathrm{NS}} e^{-[\varepsilon_{p_1} + \varepsilon_{p_2}]/T} \ . \tag{3.23}$$

The explicit expressions for $c_n(T, \eta)$ are

$$c_0(T, \eta) = \sum_q |\langle q|\sigma_0^z|0\rangle|^2 \left[1 - e^{-\varepsilon_q/T}\right] \frac{4\eta\varepsilon_q}{[\varepsilon_q^2 + \eta^2]^2} \ ,$$

$$c_1(T, \eta) = \sum_{p_1 < p_2} \sum_q |\langle p_1, p_2|\sigma_0^z|q\rangle|^2 \left[e^{-\varepsilon_q/T} - e^{-(\varepsilon_{p_1}+\varepsilon_{p_2})/T}\right] \frac{4\eta(\varepsilon_{p_1} + \varepsilon_{p_2} - \varepsilon_q)}{[(\varepsilon_{p_1} + \varepsilon_{p_2} - \varepsilon_q)^2 + \eta^2]^2} \ ,$$

$$c_2(T, \eta) = \sum_{p_1 < p_2 < p_3} \sum_{q_1 < q_2} |\langle p_1, p_2, p_3|\sigma_0^z|q_1, q_2\rangle|^2 \left[e^{-(\varepsilon_{q_1}+\varepsilon_{q_2})/T} - e^{-(\varepsilon_{p_1}+\varepsilon_{p_2}+\varepsilon_{p_3})/T}\right]$$

$$\times \frac{4\eta(\varepsilon_{p_1} + \varepsilon_{p_2} + \varepsilon_{p_3} - \varepsilon_{q_1} - \varepsilon_{q_2})}{[(\varepsilon_{p_1} + \varepsilon_{p_2} + \varepsilon_{p_3} - \varepsilon_{q_1} - \varepsilon_{q_2})^2 + \eta^2]^2}, \tag{3.24}$$

where the form factors are given in Eqn (2.4). Note that $c_0(T, \eta) \to 0$ as $\eta \to 0$ because it is not possible to satisfy the energy conservation delta function. Also in this limit, $c_1(T, \eta) \to c_1(T)$ computed in Eq. (3.14). On the other hand $c_1(T)$ vanishes for $3 < h < 5$ which implies that in this range of magnetic fields no "disconnected" contributions arise in Eq. (3.21) and we simply have $c_2(T) = \lim_{\eta \to 0} c_2(T, \eta)$. It is then straightforward to turn sums into integrals and we examine some properties of the resulting expression for $c_2(T)$ in Appendix A. By contrast, for $1 < h < 3$ $c_2(T, \eta)$ diverges with system size and the disconnected contributions in (3.21) need to be taken into account in order to obtain a finite expression. In principle it is possible to obtain a multiple contour integral representation for $c_2(T)$, but here we confine ourselves to a numerical evaluation of the momentum sums. We proceed as follows:

1. We evaluate $c_n(T, \eta)$ for several values of η and system sizes up to $L = 256$. We require η to be sufficiently large so that the finite-size corrections are negligible for our largest system sizes. We find that $\eta \approx 0.1$ is an appropriate order of magnitude.

2. We numerically extrapolate our results to $\eta = 0$ using a third order polynomial.

A useful check on this procedure is obtained by carrying it out for $c_1(T)$ and comparing it to the numerically evaluated expression (3.14), which is the result in the thermodynamic limit at $\eta \to 0$.

Results for $c_2(T)$ for $h = 1.5$ are shown in Fig. 3, where we compare extrapolations for system sizes $L = 144$ and $L = 192$.
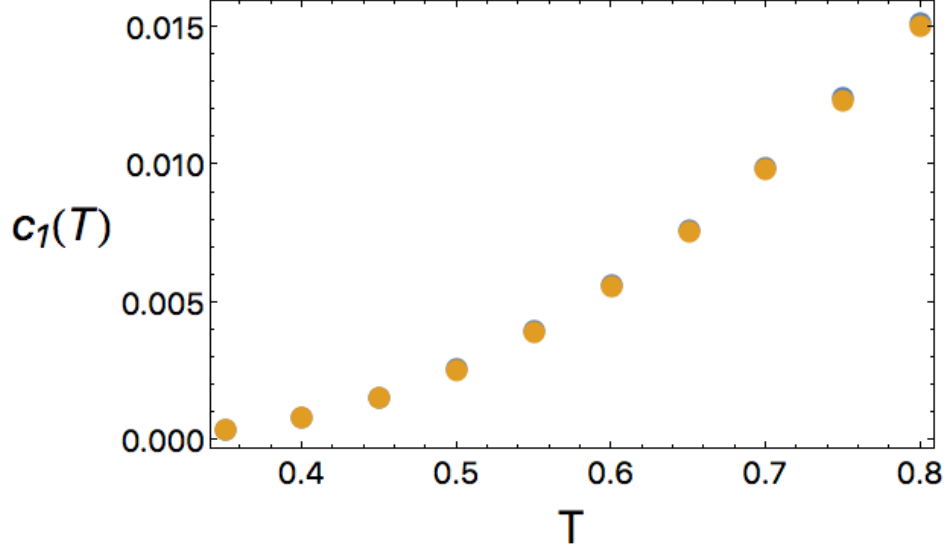
FIG. 2. $c_1(T)$ for $h = 1.5$ and several temperatures. The thermodynamic limit result (blue dots) is seen to be in good agreement with the extrapolation of numerical results for $L = 192$ and $0.1 \leqslant \eta \leqslant 0.115$ (yellow dots).
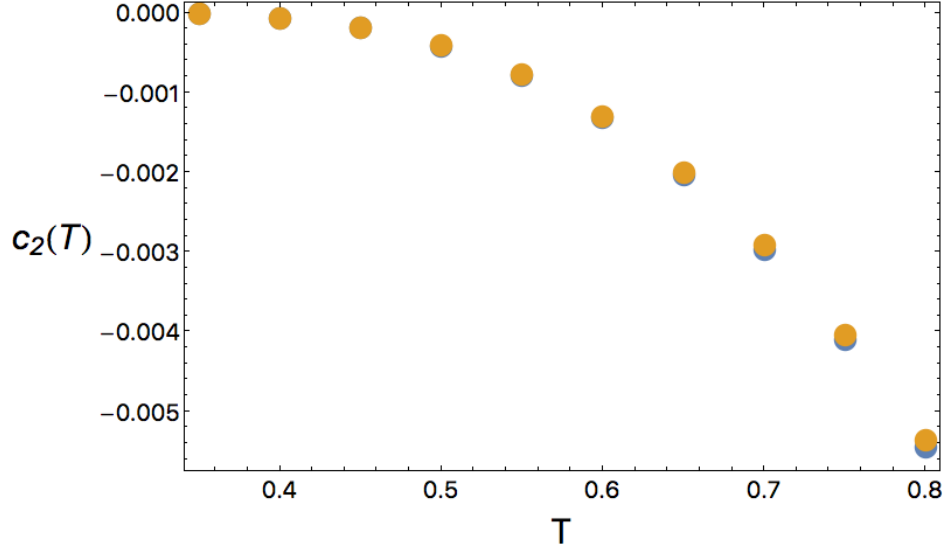

FIG. 3. $c_2(T)$ for $h = 1.5$ and several temperatures. The results of extrapolating numerical results for $0.1 \leqslant \eta \leqslant 0.115$ and $L = 144$ are in good agreement with those for $L = 192$.

IV. QUANTUM CRITICALITY

In this section we consider the approach to the quantum critical point at $h = 1$ in Fig. 1. It is useful to first review the analysis on the ferromagnetic side, $h < 1$, which was presented in Ref. 8.

Then as $\Delta \ll J$, the $1/T_1$ rate obeys the universal scaling form

$$\frac{1}{T_1} = |a_{hf}|^2 \frac{Z}{T^{3/4}} \Phi_1(\Delta/T) \quad , \quad h < 1 \quad , \quad T, \Delta \ll J , \tag{4.1}$$

where Z is a non-universal constant, while Φ_1 is a universal function describing the crossovers between the quantum critical and renormalized classical regions. For the nearest-neighbor Ising model in Eq. (2.1) we take $Z = J^{-1/4}$ for our normalization of Φ_1. While other microscopic models will have different values of Z, the function $\Phi_1(\Delta/T)$ is independent of the specific microscopic Hamiltonian. The limiting forms for Φ_1 in the two regimes are known exactly:

$$\Phi_1(\Delta/T) = \begin{cases} 2.1396\ldots & , \; \Delta \ll T \ll J \\ \pi(\Delta/T)^{1/4} e^{\Delta/T} & , \; T \ll \Delta \ll J \end{cases} . \tag{4.2}$$

Furthermore, these theoretical predictions were found to be in good agreement with experimental observations [8].

Now let us examine the paramagnetic phase $h > 1$. As in Eq. (4.1), the scaling form is

$$\frac{1}{T_1} = |a_{hf}|^2 \frac{Z}{T^{3/4}} \Phi_2(\Delta/T) \quad , \quad h > 1 \quad , \quad T, \Delta \ll J , \tag{4.3}$$

is expected to describe the crossovers in the NMR relaxation between the quantum disordered and quantum critical regimes. Matching with Eq. (4.1) in the quantum critical regime we have

$$\Phi_2(\Delta/T) = 2.1396\ldots \quad , \quad \Delta \ll T \ll J . \tag{4.4}$$

For the form of Φ_2 in the quantum disordered regime, we examine only the leading term in Eq. (3.19) in the limit $T \ll \Delta \ll J$. In this limit, the fermion dispersion in Eq. (2.2) takes a relativistic form

$$\varepsilon_p = \sqrt{\Delta^2 + c^2 p^2} \tag{4.5}$$

with $c = 2J$. We evaluate the other parameters introduced above Eq. (3.19) for this dispersion and find

$$m = \Delta/c^2 \quad , \quad p_0 = \sqrt{3}\Delta/c \quad , \quad v = \sqrt{3}c/2 . \tag{4.6}$$

Finally, inserting in Eq. (3.19) we obtain

$$\frac{1}{T_1} = |a_{hf}|^2 \frac{3\sqrt{3}T^2}{2\pi J^{1/4}\Delta^{11/4}} e^{-2\Delta/T} \quad , \quad T \ll \Delta \ll J, \; h > 1 \tag{4.7}$$

This result is compatible with the scaling form in Eq. (4.3), and we have

$$\Phi_2(\Delta/T) = \frac{3\sqrt{3}}{2\pi} \left(\frac{T}{\Delta}\right)^{11/4} e^{-2\Delta/T} \quad , \quad T \ll \Delta \ll J . \tag{4.8}$$

Note that the result in Eq. (4.8) applies to a generic ferromagnetic quantum Ising chain near its transverse field quantum critical point, and not just the nearest-neighbor model.
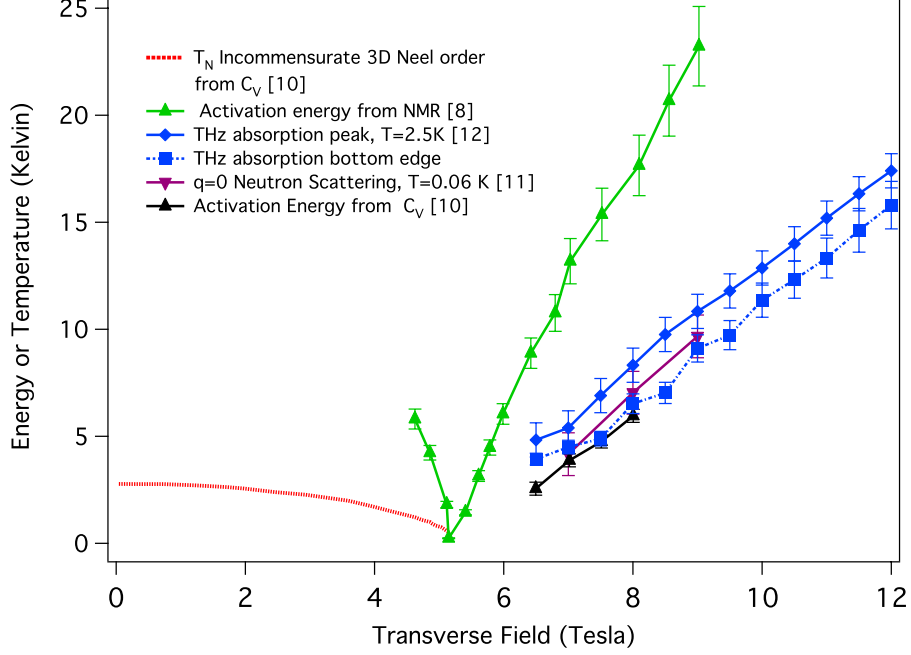
10

FIG. 4. Phase diagram and energy scales of the Ising chain system $CoNb_2O_6$ as a function of transverse field. Energy scales from different experimental probes as well as the transition temperature of the 3D incommensurate Neel order are given. The transition is to a state with ferromagnetic chains that are ordered antiferromagetically in the b. On the paramagnetic side of the transition, one can see an excellent agreement between various spectroscopic probes (THz absorption [12] and inelastic neutron scattering [11] and heat capacity [10]). In contrast one can see clearly that the gap extracted from the temperature dependence of the NMR spin relaxation time is approximately twice as large [8].

V.   EXPERIMENTS

As mentioned above $CoNb_2O_6$ has been discovered to be an almost ideal realization of a 1D ferromagnetic Ising chain [5]. It is quasi-1D material characterized by zig-zag chains of Co^{+2} ions with effective spin $1/2$ moments. The spins lie in the ac plane at an angle of $\pm 31°$ to the $c-$axis [13, 14] with the chains extending along the $c-$direction. A dominant ferromagnetic exchange between nearest-neighbor Co^{+2} ions along the c axis cause strong 1D ferromagnetic correlations to develop below $\sim$25 K [15]. At zero transverse field, weak AF inter-chain exchange interactions stabilize an incommensurate spin-density waves at 2.95 K along the b-direction with a temperature-dependent ordering wave vector $\mathbf{Q}$, and then a commensurate spin-density wave at 1.97 K. But at temperatures above these scales at zero field (and at temperatures much lower near the 1D quantum critical point (QCP)), the system can be described as a 1D Ising system. The effective

1D phase transition to a quantum disordered phase has been inferred to be at the relatively modest critical transverse field of 5.2 T in the b direction. Note that the 3D phase is believed to extend out slightly past the effective 1D QCP, a feature necessary for the observation of "kink" bound states in the spectrum near the critical point [5].

A number of measurements have been been made of the various energy scales on both sides of the transition of the 1D QCP in $CoNb_2O_6$. We will concentrate on the paramagnetic regime. As shown in Fig. 4 neutron scattering [11] and THz absorption [12] experiments have given evidence for a $q = 0$ (or symmetry equivalent) mode which increases in energy roughly linearly with field from the critical point. This may be identified straightforwardly with the zone center excitation described by Eq. 2.2. Heat capacity experiments have also been performed [10] and data fit to the nearest-neighbor Ising model. As seen in Fig. 4, the extracted gap scale from heat capacity is in excellent agreement with the spectroscopic probes. In contrast to these experiments, the scale of the lowest energy excitation extracted from the temperature dependence of the $1/T_1$ in NMR is greater by approximately a factor of two than the other probes. As explained above, this data was fit to a activated functional form which was effectively $1/T_1 \sim \exp(-\Delta_{NMR}/T)$. However, we have shown here that near the critical point the expectation is in fact $1/T_1 \sim \exp(-2\Delta/T)$. This means that the activation energy scale from $1/T_1$ will be double that extracted from the other probes. This is precisely as observed experimentally. Also note that the differences between energy scales are far bigger than anything that could be explained by inter-chain couplings or 1D vs. 3D regimes of behavior. The coupling in the transverse b direction has been found to be smaller than $1/60$ of J [7]. At low temperature on the paramagnetic side of the transition, this gives a minimum of the dispersion at finite q_b, but except very near the critical point this band width in directions perpendicular to the chain is a very small fraction of Δ [7]. The third direction has frustrated antiferromagnetic couplings and has even smaller effect on the dispersions (although it is presumably responsible for stabilizing different magnetically ordered states at low transverse field [16]). The scenario put forward in the current work comes with a distinct prediction. At fields three times the critical field $1/T_1$ should crossover to a form that goes as $\exp(-3\Delta/T)$ e.g. a much faster dependence. This is at fields greater than 15.6 T in $CoNb_2O_6$ and should be easily testable.

VI. CONCLUSIONS

The quantum Ising chain has been an essential model to understand the low frequency, non-zero temperature dynamics of a strongly interacting system [2, 3, 17]. The integrability of the model allows for exact solutions, and yet many local observables exhibit generic dissipative dynamics at long times. Here we have examined the NMR relaxation rates in the quantum disordered region.

It is given by the imaginary part of the local spin susceptibility, at frequencies far below the quasi-particle gap, Δ. Therefore it is not directly amenable to a quasi-classical computation involving collisions of a dilute gas of quasiparticles [2]. Instead, we showed here that it is dominated by rare processes in which one quasiparticle has sufficient energy to decay into two quasiparticles (and vice versa) near the nucleus. Consequently we found that the NMR relaxation is suppressed by a thermal Boltzmann factor of $\exp(-2\Delta/T)$ for not too large a transverse field, $1 < h < 3$ (the suppression is stronger for larger h). We also computed the precise prefactor of this exponential for the nearest-neighbor Ising chain, and its universal form near the quantum critical point. Finally we compared our results to the experimental probes. The scenario put forth here is in excellent agreement with the experimental results. Spectroscopic and thermodynamic probes show agreement as to the size of the gap, whereas $1/T_1$ from NMR shows an activation energy, which is approximately twice as large.

Acknowledgements

Appendix A: Evaluation of $e^{-3\Delta/T}$ contribution

The expression for $c_2(T, \eta)$ in Eq. (3.24) can be written in the limit $T \to 0$ as

$$c_2(T, \eta) = -\frac{2\pi}{2!3!T} \int_{-\pi}^{\pi} \frac{dk_1 dk_2 dq_1 dq_2 dq_3}{(2\pi)^5} |_{NS}\langle k_1 k_2 | \sigma_0^z | q_1 q_2 q_3 \rangle_R|^2 e^{-(\varepsilon_{q_1} + \varepsilon_{q_2} + \varepsilon_{q_3})/T}$$
$$\times \delta(\varepsilon_{k_1} + \varepsilon_{k_2} - \varepsilon_{q_1} - \varepsilon_{q_2} - \varepsilon_{q_3}), \tag{A1}$$

where the factorials are combinatoric factors from converting the sums to integrals. From Eq. (2.4), the form factor is

$$
|_{NS}\langle k_1 k_2 | \sigma_0^z | q_1 q_2 q_3 \rangle_R|^2 = \frac{(4J^2 h)^{\frac{1}{2}} |1 - h^2|^{\frac{1}{4}}}{\varepsilon_{k_1} \varepsilon_{k_2} \varepsilon_{q_1} \varepsilon_{q_2} \varepsilon_{q_3}}
$$

$$
\times \left(\frac{\sin\left(\frac{k_1 - k_2}{2}\right) \sin\left(\frac{q_1 - q_2}{2}\right) \sin\left(\frac{q_1 - q_3}{2}\right) \sin\left(\frac{q_2 - q_3}{2}\right)}{\sin\left(\frac{k_1 - p_1}{2}\right) \sin\left(\frac{k_1 - q_2}{2}\right) \sin\left(\frac{k_1 - q_3}{2}\right) \sin\left(\frac{k_2 - q_1}{2}\right) \sin\left(\frac{k_2 - q_2}{2}\right) \sin\left(\frac{k_2 - q_3}{2}\right)} \right)^2
$$

$$
\times \left(\frac{(\varepsilon_{k_1} + \varepsilon_{q_1})(\varepsilon_{k_1} + \varepsilon_{q_2})(\varepsilon_{k_1} + \varepsilon_{q_3})(\varepsilon_{k_2} + \varepsilon_{q_1})(\varepsilon_{k_2} + \varepsilon_{q_2})(\varepsilon_{k_2} + \varepsilon_{q_3})}{4(\varepsilon_{k_1} + \varepsilon_{k_2})(\varepsilon_{q_1} + \varepsilon_{q_2})(\varepsilon_{q_1} + \varepsilon_{q_3})(\varepsilon_{q_2} + \varepsilon_{q_3})} \right)^2 . \tag{A2}
$$

We now attempt to take the $T \to 0$ limit of Eq. (A1) in a manner similar to the analysis below Eq. (3.14). The integral is dominated by small $q_{1,2,3} \sim \sqrt{T}$. This allows us to make the following approximations

$$
\varepsilon_{q_i} \approx \frac{q_i^2}{2m} + \Delta
$$

$$
\sin\left(\frac{q_i - q_j}{2}\right) \approx \frac{q_i - q_j}{2}
$$

$$
\varepsilon_{q_1} + \varepsilon_{q_2} = 2\Delta \tag{A3}
$$

We can now write Eqn. (A2) as a product of a term containing the q_1, q_2, and q_3 dependence, with one containing the k_1 and k_2 dependence. The $q_{1,2,3}$ integral is sharply peaked about momenta $\sim \sqrt{T}$ in the q_1, q_2, q_3 plane, so we can extend the limit of integration over these momenta out to infinity giving us the following

$$
c_2(T, \eta) \approx -\frac{e^{-3\Delta/T} 4\pi J (h^2 |1 - h^2|)^{\frac{1}{4}}}{3!2!\Delta^9 2^{16} T} \int_{-\pi}^{\pi} \frac{dk_1 dk_2}{(2\pi)^2} \frac{((\varepsilon_{k_1} + \Delta)^3 (\varepsilon_{k_2} + \Delta)^3)^2}{\varepsilon_{k_1} \varepsilon_{k_2} (\varepsilon_{k_1} + \varepsilon_{k_2})^2}
$$

$$
\times \left(\frac{\sin\left(\frac{k_1 - k_2}{2}\right)}{\sin^3\left(\frac{k_1}{2}\right) \sin^3\left(\frac{k_2}{2}\right)} \right)^2 \delta(\varepsilon_{k_1} + \varepsilon_{k_2} - 3\Delta)
$$

$$
\times \int_{-\infty}^{\infty} \frac{dq_1 dq_2 dq_3}{(2\pi)^3} ((q_1 - q_2)(q_1 - q_3)(q_2 - q_3))^2 e^{-(q_1^2 + q_2^2 + q_3^2)/2mT} . \tag{A4}
$$

The $q_{1,2,3}$ integrals evaluate to

$$
\int_{-\infty}^{\infty} \frac{dq_1 dq_2 dq_3}{(2\pi)^3} (q_1 - q_2)^2 (q_1 - q_3)^2 (q_2 - q_3)^2 e^{-(q_1^2 + q_2^2 + q_3^2)/2mT} = 12(2\pi)^{-\frac{3}{2}} (mT)^{\frac{9}{2}} , \tag{A5}
$$

which yields

$$
c_2(T, \eta) \approx -\frac{e^{-3\Delta/T} 2J (h^2 |1 - h^2|)^{\frac{1}{4}} (mT)^{\frac{9}{2}}}{\Delta^9 (2\pi)^{\frac{1}{2}} 2^{16} T}
$$

$$
\times \int_{-\pi}^{\pi} \frac{dk_1 dk_2}{(2\pi)^2} \frac{((\varepsilon_{k_1} + \Delta)^3 (\varepsilon_{k_2} + \Delta)^3)^2}{\varepsilon_{k_1} \varepsilon_{k_2} (\varepsilon_{k_1} + \varepsilon_{k_2})^2} \frac{\sin^2\left(\frac{k_1 - k_2}{2}\right)}{\sin^6\left(\frac{k_1}{2}\right) \sin^6\left(\frac{k_2}{2}\right)} \delta(\varepsilon_{k_1} + \varepsilon_{k_2} - 3\Delta) \tag{A6}
$$

14

Now we have to perform the final integrals over $k_{1,2}$. Because of the singularities in the form factors at small momenta, the integrals have infrared divergencies which need to be treated differently depending upon the value of h.

For $3 < h < 5$, the energy conservation delta function in Eq. (A6) prevents a divergence. The argument of the delta function does not vanish when either $k_1 = 0$ or $k_2 = 0$. Consequently, the $k_{1,2}$ integrals are finite, and we obtain

$$c_2(T, \eta) \sim T^{7/2} e^{-3\Delta/T} \quad , \quad T \ll \Delta \quad , \quad 3 < h < 5 \, , \tag{A7}$$

so that the contribution to $1/T_1$ is $\sim T^{9/2} e^{-3\Delta/T}$.

However, for $1 < h < 3$, there are divergences in Eq. (A6). The divergences are present when either $k_1 = 0$ or $k_2 = 0$. So let us consider the form of Eq. (A6) when both k_1 are k_2 small. After suitable rescaling of momenta, we obtain an expression of the form

$$c_2(T, \eta) \sim T^{7/2} e^{-3\Delta/T} \int dk_1 dk_2 \frac{(k_1 - k_2)^2}{k_1^6 k_2^6} \delta\left((k_1^2 + 1)^{1/2} + (k_2^2 + 1)^{1/2} - 3\right) \, . \tag{A8}$$

This integral has an effective divergence $\sim \int dk/k^6$. As we discussed below Eq. (3.24), this divergence will be cancelled by the other terms in Eq. (3.21). A conjectured estimate is obtained by cutting off the divergence at $k \sim \sqrt{T}$, which leads to $c_2(T) \sim T e^{-3\Delta/T}$ and therefore a contribution to $1/T_1$ which is $\sim T^2 e^{-3\Delta/T}$.

---

[1] S. Sachdev, *Quantum Phase Transitions*, 1st ed. (Cambridge University Press, Cambridge, UK, 1999).

[2] S. Sachdev and A. P. Young, "Low Temperature Relaxational Dynamics of the Ising Chain in a Transverse Field," Phys. Rev. Lett. **78**, 2220 (1997), cond-mat/9609185.

[3] F. H. L. Essler and R. M. Konik, "Finite-temperature dynamical correlations in massive integrable quantum field theories," J. Stat. Mech. **9**, 09018 (2009), arXiv:0907.0779 [cond-mat.str-el].

[4] N. Iorgov, V. Shadura, and Yu. Tykhyy, "Spin operator matrix elements in the quantum Ising chain: fermion approach," J. Stat. Mech. **1102**, P02028 (2011), arXiv:1011.2603 [cond-mat.stat-mech].

[5] R. Coldea, D. A. Tennant, E. M. Wheeler, E. Wawrzynska, D. Prabhakaran, M. Telling, K. Habicht, P. Smeibidl, and K. Kiefer, "Quantum Criticality in an Ising Chain: Experimental Evidence for Emergent E$_8$ Symmetry," Science **327**, 177 (2010), arXiv:1103.3694 [cond-mat.str-el].

[6] H. Bernien, S. Schwartz, A. Keesling, H. Levine, A. Omran, H. Pichler, S. Choi, A. S. Zibrov, M. Endres, M. Greiner, V. Vuletić, and M. D. Lukin, "Probing many-body dynamics on a 51-atom quantum simulator," Nature **551**, 579 (2017), arXiv:1707.04344 [quant-ph].

[7] I. Cabrera, J. D. Thompson, R. Coldea, D. Prabhakaran, R. I. Bewley, T. Guidi, J. A. Rodriguez-Rivera, and C. Stock, "Excitations in the quantum paramagnetic phase of the quasi-one-dimensional Ising magnet CoNb2O6 in a transverse field: Geometric frustration and quantum renormalization effects," Phys. Rev. B **90**, 014418 (2014), arXiv:1402.7355 [cond-mat.str-el].

[8] A. W. Kinross, M. Fu, T. J. Munsie, H. A. Dabkowska, G. M. Luke, S. Sachdev, and T. Imai, "Evolution of Quantum Fluctuations Near the Quantum Critical Point of the Transverse Field Ising Chain System $CoNb_2O_6$," Phys. Rev. X **4**, 031008 (2014), arXiv:1401.6917 [cond-mat.str-el].

[9] C. M. Morris, R. Valdés Aguilar, A. Ghosh, S. M. Koohpayeh, J. Krizan, R. J. Cava, O. Tchernyshyov, T. M. McQueen, and N. P. Armitage, "Hierarchy of Bound States in the One-Dimensional Ferromagnetic Ising Chain $CoNb_2O_6$ Investigated by High-Resolution Time-Domain Terahertz Spectroscopy," Phys. Rev. Lett. **112**, 137403 (2014), arXiv:1312.4514 [cond-mat.str-el].

[10] T. Liang, S. M. Koohpayeh, J. W. Krizan, T. M. McQueen, R. J. Cava, and N. P. Ong, "Heat capacity peak at the quantum critical point of the transverse Ising magnet $CoNb_2O_6$," Nature Communications **6**, 7611 (2015), arXiv:1405.4551 [cond-mat.str-el].

[11] N. J. Robinson, F. H. L. Essler, I. Cabrera, and R. Coldea, "Quasiparticle breakdown in the quasi-one-dimensional Ising ferromagnet $CoNb_2O_6$," Phys. Rev. B **90**, 174406 (2014), arXiv:1407.2794 [cond-mat.str-el].

[12] J. Viirok, D. Hüvonen, T. Room, U. Nagel, C. Morris, S. Koohpayeh, T. McQueen, J. Krizan, R. Cava, and N. Armitage, "THz Spectroscopy of the Quantum Criticality in a Transverse Field Ising Chain Compound $CoNb_2O_6$," to be submitted (2018).

[13] C. Heid, H. Weitzel, P. Burlet, M. Bonnet, W. Gonschorek, T. Vogt, J. Norwig, and H. Fuess, "Magnetic phase diagram of $CoNb_2O_6$: A neutron diffraction study ," J. Mag. Mag. Mat. **151**, 123 (1995).

[14] S. Kobayashi, S. Mitsuda, and K. Prokes, "Low-temperature magnetic phase transitions of the geometrically frustrated isosceles triangular Ising antiferromagnet $CoNb_2O_6$," Phys. Rev. B **63**, 024415 (2000).

[15] T. Hanawa, K. Shinkawa, M. Ishikawa, K. Miyatani, K. Saito, and K. Kohn, "Anisotropic Specific Heat of $CoNb_2O_6$ in Magnetic Fields," J. Phys. Soc. Jpn. **63**, 2706 (1994).

[16] S. Lee, R. K. Kaul, and L. Balents, "Interplay of quantum criticality and geometric frustration in columbite," Nature Physics **6**, 702 (2010), arXiv:0911.0038 [cond-mat.str-el].

[17] P. Calabrese, F. H. L. Essler, and M. Fagotti, "Quantum quench in the transverse field Ising chain: I. Time evolution of order parameter correlators," J. Stat. Mech. **7**, 07016 (2012), arXiv:1204.3911 [cond-mat.quant-gas].